Motexafin Gadolinium Disrupts Zinc Metabolism in Human Cancer Cell Lines

Darren Magda,[1] Philip Lecane,[1] Richard A. Miller,[1] Cheryl Lepp,[1] Dale Miles,[1] Mimi Mesfin,[1] John E. Biaglow,[2] Vincent V. Ho,[3] Danny Chawannakul,[3] Shailender Nagpal,[3] Mazen W. Karaman,[3] and Joseph G. Hacia[3]

[1]Pharmacyclics, Inc., Sunnyvale, California; [2]Department of Radiation Oncology, University of Pennsylvania, Philadelphia, Pennsylvania; and [3]Institute for Genetic Medicine, University of Southern California, Los Angeles, California

Abstract

To gain a better understanding of the mechanism of action of the metal cation–containing chemotherapeutic drug motexafin gadolinium (MGd), gene expression profiling analyses were conducted on plateau phase human lung cancer (A549) cell cultures treated with MGd. Drug treatment elicited a highly specific response that manifested in elevated levels of metallothionein isoform and zinc transporter 1 (*ZnT1*) transcripts. A549 cultures incubated with MGd in the presence of exogenous zinc acetate displayed synergistic increases in the levels of intracellular free zinc, metallothionein transcripts, inhibition of thioredoxin reductase activity, and cell death. Similar effects were observed in PC3 prostate cancer and Ramos B-cell lymphoma cell lines. Intracellular free zinc levels increased in response to treatment with MGd in the absence of exogenous zinc, indicating that MGd can mobilize bound intracellular zinc. These findings lead us to suggest that an important component of the anticancer activity of MGd is related to its ability to disrupt zinc metabolism and alter cellular availability of zinc. This class of compounds may provide insight into the development of novel cancer drugs targeting control of intracellular free zinc and the roles that zinc and other metal cations play in biochemical pathways relevant to cancer. (Cancer Res 2005; 65(9): 3837-45)

Introduction

The disruption of metal cation homeostasis can play a significant role in the development and progression of cancer (1–5). Intracellular levels of zinc, in particular, are known to regulate biological pathways involved in carcinogenesis (6–10) and in modulating the effectiveness of the immune system (11). For example, intracellular zinc levels can modulate mitogen-activated protein kinase, extracellular signal-regulated kinase, protein kinase C, and nuclear factor κB signaling pathways (6–10). Zinc also plays a major role in modulating the effectiveness of the immune system, in part through its effect on the expression of genes associated with the amplification of the Th1 immune response (11). In addition, genes involved in intracellular zinc trafficking (i.e., metallothionein gene family members) are frequently either over- or underexpressed in a variety of tumors (3–5) and may be involved in tumor growth regulation (12).

Interestingly, several classes of chemotherapeutic agents contain metal cations that are essential for their biological activities (13, 14). For example, motexafin gadolinium (MGd, Xcytrin, Fig. 1*A*), an expanded porphyrin containing the lanthanide cation gadolinium, is currently in clinical trials for the treatment of several forms of cancer (15–23). MGd is an electron-affinic compound that mediates electron transfer from a variety of intracellular reducing species, such as ascorbate, NADPH, and thiols, to oxygen to form superoxide and hydrogen peroxide (20–23). Although the relative importance of the impact MGd has on each of these intracellular processes is unknown, it is interesting to note that the most facile redox reaction seems to occur with vicinal thiols, a chemical motif most commonly associated with the binding of zinc (22).

Here, we generated gene expression profiles of plateau phase A549 cell cultures treated with MGd for the purpose of gaining insights into the mechanisms of its biological activity. A remarkably specific cellular response to drug treatment was observed, which resulted in the marked induction of transcript levels of genes that play major roles in controlling free zinc levels. We found that MGd increased intracellular free zinc levels, modulated the cellular toxicity of zinc, and inhibited cellular bioreductive activity in human cancer cell lines. Based on our findings, we propose a mechanism of MGd activity and suggest that disregulation of zinc homeostasis represents a potentially important strategy for anticancer therapy.

Materials and Methods

Cells and cell culture reagents. A549 lung cancer, PC3 prostate cancer, and Ramos B-cell lymphoma lines were obtained from the American Type Culture Collection (Manassas, VA). Unless otherwise indicated, all cell culture reagents were purchased from Invitrogen (Carlsbad, CA). Cells were cultured in RPMI 1640 supplemented with 20 mmol/L HEPES, 2 mmol/L L-glutamine, 10% fetal bovine serum (SH30021, Hyclone, Logan, UT) and antibiotics (200 units/mL penicillin and 200 μg/mL streptomycin). Unless specified otherwise, plateau phase cultures of A549 and PC3 cells were used. The cell density of Ramos cultures was maintained between 0.2×10^6 and 1×10^6 cells/mL. Motexafin gadolinium (MGd) was prepared as a 2 mmol/L (2.3 mg/mL) formulation in 5% aqueous mannitol. Gadolinium acetate, cadmium chloride, and zinc acetate were purchased from Aldrich Chemical (St. Louis, MO) and prepared as 2 mmol/L formulations in 5% aqueous mannitol. The zinc salt of 1-hydroxypyridine-2-thione (Sigma Chemical, St. Louis, MO) was formulated as a 20 mmol/L stock solution in DMSO. Plateau phase cultures were chosen to obviate any effect that drug treatment might have on cell cycle, to reduce experimental variability, and to examine the effect of the drug in a system that might better mimic conditions extant in the tumor microenvironment (24). In other cases, exponential phase cultures were used to assess the effect of treatment on proliferation.

Gene expression profiling. A549 human lung cancer cells (6.5×10^5 cells per T-162 flask in 45 mL complete RPMI 1640) were seeded 10 days

Note: Supplementary data for this article are available at Cancer Research Online (http://cancerres.aacrjournals.org/).

Requests for reprints: Joseph G. Hacia, Institute for Genetic Medicine, University of Southern California, 2250 Alcazar Street, IGM 240, Los Angeles, CA 90089. Phone: 323-442-3030; Fax: 323-442-2764; E-mail: hacia@hsc.usc.edu.

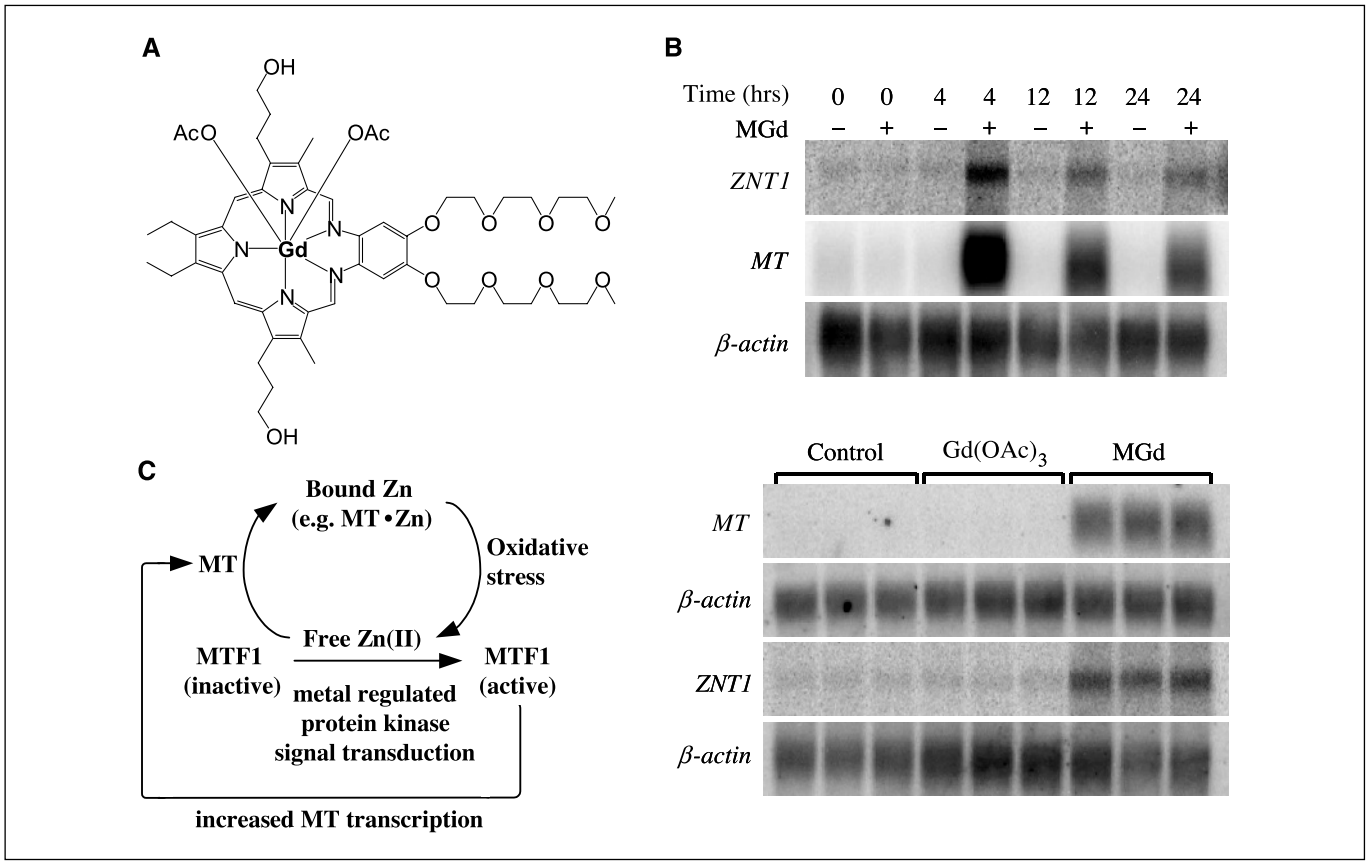

Figure 1. MGd treatment of A549 cultures. *A,* chemical structure of MGd. *B,* MGd up-regulation of RNA expression levels as determined by Northern hybridization in (*top*) representative microarray samples or (*bottom*) plateau phase A549 cultures treated for 4 hours with control vehicle (*Control*), gadolinium acetate [*Gd(OAc)$_3$*, 5 μmol/L], or MGd (50 μmol/L). *C,* schematic diagram of metallothionein (*MT*) gene regulation in response to oxidative stress.

before treatment of noncycling plateau phase cultures with MGd. At 4, 12, or 24 hours before RNA isolation, MGd (50 μmol/L final concentration) or control (5% mannitol) solution was added to the cultures. Each time course experiment was done in triplicate. After incubation, all cultures were washed once with PBS and total RNA was (25) subjected to analysis on Affymetrix (Santa Clara, CA) U133A microarrays, designed to interrogate the relative abundance of over 15,000 human genes as described (25).

We used Microarray Suite version 5.0 software (Affymetrix) to generate raw gene expression scores and normalized the relative hybridization signal from each experiment as described (25). All gene expression scores were set to a minimum value of 100 to minimize noise associated with less robust measurements of rare transcripts. The permutation-based significance analysis of microarrays (SAM) was used to determine genes differentially expressed in response to MGd treatment compared with the control 5% mannitol–treated cultures (0.125% final) at each time point (26). We report all genes at least 2-fold differentially expressed with a <1% false discovery rate in response to MGd treatment (Table 1). The use of lower fold change cutoffs (down to 1.01-fold) in SAM analysis did not identify any additional differentially expressed genes. All raw fluorescent intensity values from microarray experiments are available in the Supplementary Materials. All cell files are available at http://hacialab.usc.edu/supplement/magda_etal_2005/.

Northern blot analysis. Plateau phase cultures of A549 cells were prepared as described above, except that T-25 flasks were used and the number of cells initially plated scaled accordingly. Cultures were treated with 50 μmol/L MGd, 5 μmol/L gadolinium acetate or 5% mannitol for 4 hours, whereupon cultures were washed twice with PBS and RNA harvested as above. Alternatively, 7-day plateau phase A549 or PC3 cultures were treated with 50 μmol/L MGd, 50 to 100 μmol/L zinc acetate, 50 μmol/L cadmium chloride, or 5% mannitol for 24 hours (A549) or 4 hours (PC3) before washing and RNA analysis. Exponential phase Ramos cultures were treated for 6 hours. Northern blots were conducted and analyzed as described (25). Radiolabeled metallothionein probe, designed to bind to a 113-bp region of 3′ untranslated region (UTR) sequences from multiple metallothionein gene family members, was generated using 5′-ATGGACCCCAACTGCTCCTG-3′ (forward) and 5′-GGGCAGCAGGAGCAGCAGCT-3′ (reverse) PCR primers and the NEBlot kit (New England Biolabs, Inc., Beverly, MA). Radiolabeled *ZnT1* probe was generated in a similar fashion using 5′-TGCTGGAAGCA-GAATCATTG-3′ (forward) and 5′-TGCTAACTGCTGGGGTCTTT-3′ (reverse) primers.

Cellular viability. Cell viability was determined by using propidium iodide flow cytometric analysis. Cells from plateau phase cultures grown in T-25 flasks were harvested as described above, except that cells present in the growth medium and wash solution were isolated by centrifugation and included in the analysis. Cells were resuspended in 1 mL PBS, an aliquot of 3×10^5 cells transferred to a 4-mL tube, and the cells isolated by centrifugation. Cell pellets were resuspended in PBS supplemented with 2 μg/mL propidium iodide (Sigma), incubated for 5 minutes at ambient temperature, and subjected to flow cytometric analysis. Flow cytometry was done on a FACSCalibur instrument and data were analyzed using the CellQuest Pro software package (BD Biosciences, San Jose, CA).

Cellular proliferation. The proliferation of exponential phase cultures of A549 and PC3 cells was assessed by formazan reduction (27). In brief, A549 (2,000 cells per well) or PC3 (4,000 cells per well) cells were seeded on 96-well microtiter plates and allowed to adhere overnight. Stock solutions of MGd or $ZnOAc_2$ in medium were added and plates were incubated at 37°C under a 5% CO_2/95% air atmosphere. After 24 hours, medium was replaced with fresh medium. After 2 additional days, medium was exchanged for fresh medium (150 μL/well) supplemented with the

tetrazolium dye, 3-(4,5-dimethylthiazol-2-yl)-2,5-diphenyltetrazolium bromide (MTT, Sigma Chemical, 0.5 mg/mL). Plates were incubated at 37°C and viable cells measured as described (21). Ramos cell cultures were seeded at an initial cell density of 2.5×10^5 cells/mL in 7 mL medium. T-25 flasks were sampled at indicated time intervals and counted using a Coulter counter.

Lipoate reduction. Thioredoxin reductase activity was assessed by measuring the rate of lipoate reduction (28). In brief, A549 or PC3 cells (10,000 cells per well) were plated on 96-well plates and allowed to adhere overnight and grow two additional days until confluent. Cells were treated with MGd, zinc, or 5% mannitol for 2 to 4 hours, as indicated. Medium was removed, cells were washed with HBSS, and a solution of 5 mmol/L lipoic acid and 1 mmol/L 5,5′-dithiobis(2-nitrobenzoic acid) in HBSS (100 μL per well) was added. Plates were incubated at ambient temperature in the dark. At chosen time intervals, plate absorbance was measured at 405 minus 650 nm. Plate absorbances were normalized to wells containing neither exogenous zinc nor texaphyrin complex to allow plate-to-plate comparison. In some experiments, buthionine sulfoximine (BSO, 100 μmol/L) was added 24 hours before MGd or zinc treatment to inhibit any contribution to lipoate reduction made by glutathione-dependent pathways (28). Actinomycin D (2.5 μg/mL) or cycloheximide (10 μg/mL), where present, was added 1 hour before texaphyrin or zinc treatment. Viability was checked on parallel plates using the tetrazolium dye 3-(4,5-dimethylthiazol-2-yl)-5-(3-carboxymethoxyphenyl)-2-(4-sulfophenyl)-2*H*-tetrazolium (MTS) following the manufacturers protocol (Promega Corp., Madison, WI). MTS signal was not altered by any treatment condition within the time frame of the lipoate reduction assay.

Intracellular free zinc. The concentration of intracellular free zinc was assessed using the ion-specific fluorescent probe, FluoZin-3-AM (FluoZin-3, Molecular Probes, Inc., Eugene, OR; ref. 29). Plateau phase cultures grown in T-25 flasks were treated with control 5% mannitol vehicle or zinc acetate in the presence or absence of MGd as described above, for 4 hours. After MGd treatment, cells were washed with PBS, and treated with trypsin/EDTA for 5 minutes. Complete medium was then added and the cells isolated by centrifugation. Cell pellets were washed and resuspended in PBS. An aliquot of 10^6 cells (200 μL) was removed, centrifuged, and resuspended in 100 μL of 20 μmol/L FluoZin-3 and 0.2% pluronic acid F127 (Molecular Probes) in PBS. After a 25-minute incubation under ambient conditions, cells were washed twice with PBS, resuspended in 0.5 mL PBS, and again incubated for 20 minutes. An aliquot of the cell suspension was supplemented with 2 μg/mL propidium iodide (Sigma), incubated for 5 minutes, and subjected to two-parameter flow cytometric analysis. FluoZin-3 fluorescence was measured at 530 nm in live-gated cells. As controls, a portion of mannitol-treated cells was treated with 20 μmol/L pyrithione (Sigma) and 50 μmol/L zinc acetate or with 20 μmol/L *N*,*N*,*N*′,*N*′-tetrakis(2-pyridylmethyl)ethylenediamine (Sigma) for 15 minutes, then processed and analyzed as above. These cells displayed average fluorescence intensity at 530 nm of 2,600 and 29 units, respectively. In other experiments, A549 cultures were washed, incubated with zinc acetate and MGd in serum-free medium for 4 hours, then analyzed for intracellular zinc as above. Actinomycin D (2.5 μg/mL, Calbiochem, Inc., San Diego, CA) was added 1 hour before MGd and zinc acetate where indicated.

Table 1. Differential gene regulation in response to MGd treatments

GenBank ID*	4 h†	12 h†	24 h†	Average‡	Gene name
M10943	37.1	49.2	36.7	41.0	*Metallothionein 1F*
AF078844§	39.7	47.3	30.3	39.1	*RNA helicase-related protein*
NM_005951	29.8	32.0	9.5	23.8	*Metallothionein 1H*
AF333388	21.7	23.2	9.4	18.1	*Metallothionein 1H-like*
NM_002450	23.2	20.0	10.0	17.8	*Metallothionein 1L*
NM_005952	16.5	16.2	13.5	15.4	*Metallothionein 1X*
NM_005953	9.8	8.6	7.3	8.6	*Metallothionein 2A*
NM_005950	8.0	6.0	8.7	7.6	*Metallothionein 1G*
AI972416	6.8	4.7	3.5	5.0	*Zinc transporter 1*
AL031602	4.4	3.7	4.8	4.3	Similar to *metallothionein 1E*
BF217861	2.2	2.5	1.6	2.1	*Metallothionein 1E*

*Available at http://www.ncbi.nlm.nih.gov/Entrez/index.html.
† Ratio of gene expression scores for cultures treated and not treated with 50 μmol/L motexafin gadolinium for the indicated time frame.
‡ Ratio of gene expression scores treated and not treated with 50 μmol/L motexafin gadolinium for all time frames. All genes that achieved significance using SAM criteria described in Materials and Methods are shown.
§Protein has a COOH-terminal domain similar to human metallothionein 1F.

Results

Gene expression. To assess the effects of drug on gene expression profiles, total cellular RNA was isolated from plateau phase A549 cultures treated with 50 μmol/L MGd for 4, 12, and 24 hours in triplicate and analyzed on oligonucleotide microarrays (25). Eleven genes showed at least a 2-fold differential expression in response to MGd treatment (averaged across all time frames) that reached statistical significance by SAM analysis (Table 1). The most prominent consequence of MGd treatment was the up-regulation of various metallothionein isoform transcripts at all time points. In fact, 10 of the 11 transcripts listed in Table 1 are metallothionein related. The remaining transcript, hbc647, was also up-regulated by MGd treatment at all three time points. This cDNA (30) is located 5 kb downstream of the zinc transporter 1 (*ZnT1*) gene and is likely to make up part of the 3′ UTR of this gene. Northern blot analysis confirmed the induction of metallothionein gene family members and *ZnT1* (Fig. 1*B*, *top*). These transcripts are under the control of metal-response element-binding transcription factor-1 (MTF-1; Fig. 1*C*; refs. 31–34).

Metallothionein induction by motexafin gadolinium compared with free gadolinium acetate. Metallothionein induction has been reported to occur in response to certain metal cations, including gadolinium(III), and oxidative stress (3–5, 35, 36). Therefore, we considered whether the metallothionein transcript up-regulation observed in the microarray analysis could be a consequence of free gadolinium(III) cation, released from MGd into the cell culture medium. High-performance liquid chromatography analysis of MGd stability in medium obtained from plateau phase cultures indicated that the drug seemed to be stable, with an apparent loss of only 4% after 24 hours (data not shown). Because the microarray analysis indicated strong transcript up-regulation after 4 hours of treatment with drug, we selected this time interval for further investigation of RNA transcript levels. RNA was harvested from plateau phase cultures treated with control vehicle, 50 μmol/L MGd, or 5 μmol/L gadolinium acetate for 4 hours. Northern blot analysis indicated metallothionein gene family members and *ZnT1* were induced only in cultures treated with MGd (Fig. 1*B*, *bottom*). Thus, even assuming a 10% loss of drug over the initial 4-hour incubation period, the resulting release of Gd(III) ion into the culture medium would be insufficient to induce the observed metallothionein and *ZnT1* transcript levels.

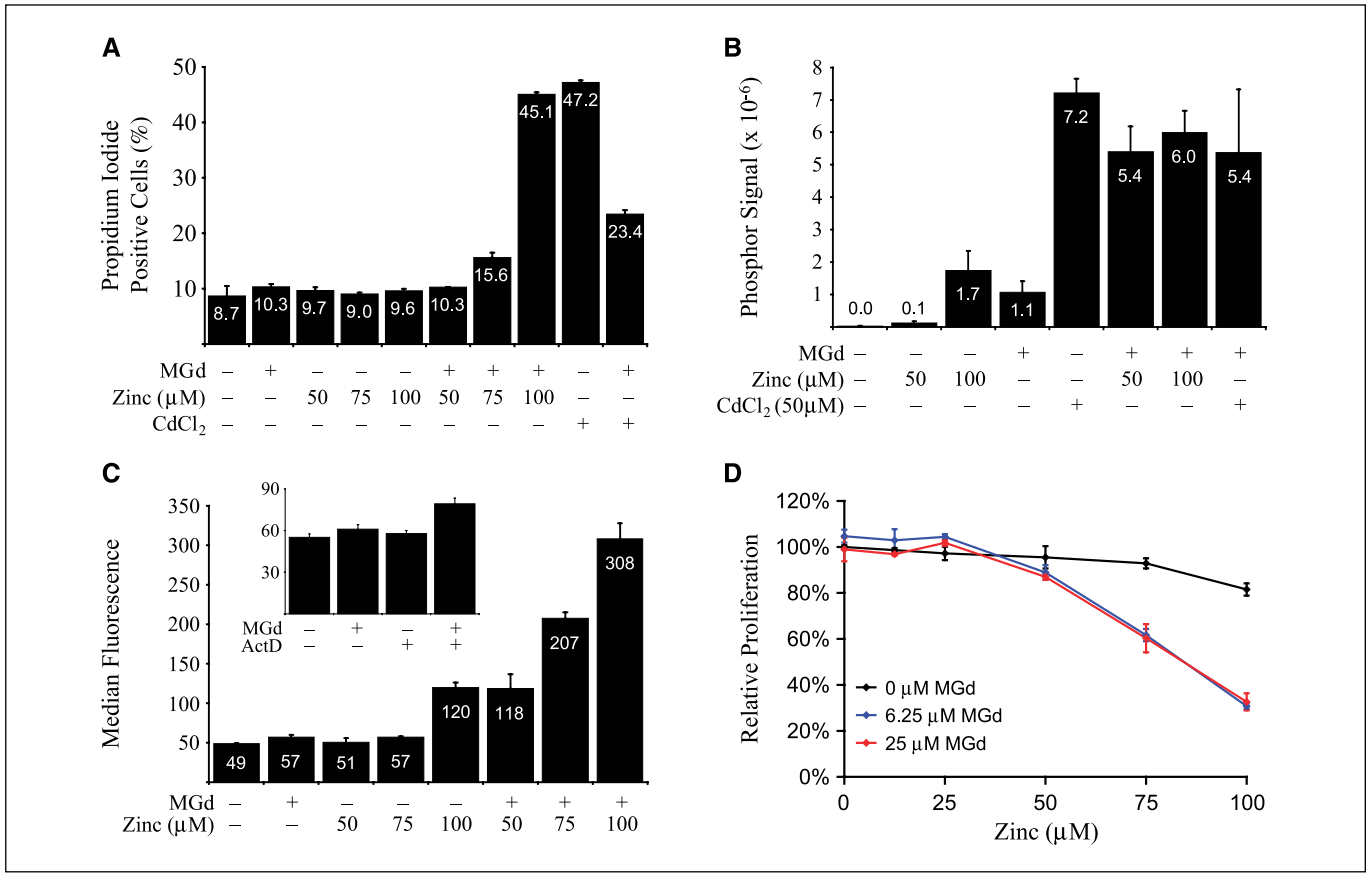

Figure 2. MGd treatment alters response of A549 cells to zinc or cadmium. *A*, cell viability as measured by propidium iodide exclusion. Plateau phase cultures were treated with zinc acetate (*Zinc*, 50-100 μmol/L), cadmium chloride (*$CdCl_2$*, 50 μmol/L), or MGd (50 μmol/L) for 24 hours in duplicate experiments. *Bars,* 1 SD. *B,* transcript levels of metallothionein family members in A549 cultures treated with MGd (50 μmol/L) and metal cations as determined by Northern blot analysis. Phosphorimager signals from metallothionein family members were normalized to those of internal β-actin controls. *C,* measurement of intracellular free zinc in A549 cells. Plateau phase cultures were treated with zinc acetate (50-100 μmol/L) or MGd (50 μmol/L) for 4 hours in duplicate experiments. *Columns,* median fluorescence at 530 nm of cells treated with FluoZin-3, as described in Materials and Methods. *Bars,* SD. *Inset,* median fluorescence of cells treated with MGd in serum-free medium in the absence and presence of 2.5 μg/mL actinomycin D (*ActD*). *D,* effect of MGd and zinc treatment on proliferation of A549 cells. Exponential growth phase cultures were treated with MGd (0, 6.25, and 25 μmol/L) and metal cation (0-100 μmol/L) for 24 hours, medium replaced, and proliferation relative to control assessed by colorimetric (MTT) assay after 72 hours. Cells treated with 12.5 and 18.75 μmol/L MGd behaved in a similar fashion to those treated with 25 μmol/L MGd (data not shown). *Bars,* SD.

Motexafin gadolinium increases sensitivity of cells to zinc acetate. The above findings indicated that MGd treatment might alter cellular response to metal cations. This could be relevant because the levels of zinc available to cultured cancer cells and to cancer cells *in vivo* may not directly coincide in all instances. To examine this possibility, A549 cultures were treated with zinc acetate (100 μmol/L) or cadmium chloride (50 μmol/L) for 24 hours in the presence or absence of 50 μmol/L MGd. Treatment with zinc acetate alone had no effect on cellular viability, as assessed by propidium iodide exclusion (Fig. 2*A*). By contrast, viability dropped from ~90% to ~55% after treatment with zinc acetate and MGd. This is dependent on treatment time because there are limited effects on cellular viability at 4 hours and only intermediate effects at 12 hours relative to 24-hour treatments (Supplementary Fig. 1). Conversely, viability after cadmium chloride treatment (~53%) was increased to ~76% by coincubation with MGd. It has been reported that metallothionein induction protects cells from cadmium chloride treatment (37, 38). The effects of zinc acetate and cadmium chloride were not altered by gadolinium acetate (50 μmol/L, data not shown).

Metallothionein induction by zinc and cadmium treatment in the presence and absence of motexafin gadolinium. RNA harvested from surviving A549 cells, treated as above, was analyzed for metallothionein transcript induction. Treatment with zinc acetate, cadmium chloride, or MGd resulted in significant increase in the levels of these RNA transcripts (Fig. 2*B*). Interestingly, cotreatment with zinc acetate and MGd led to a synergistic increase in the levels of metallothionein transcripts (Fig. 2*B*). Treatment with cadmium led to high levels of metallothionein transcription, in the presence or absence of MGd.

Intracellular free zinc is elevated in motexafin gadolinium–treated cells. The above findings indicated that MGd treatment might alter the cellular availability of zinc ion. Therefore, cultures of A549 cells were incubated with MGd and zinc for 4 hours, and cells were analyzed for free (chelatable) intracellular zinc using the ion-specific dye, FluoZin-3 (29). Treatment with 100 μmol/L zinc acetate significantly increased the cell-associated fluorescence of FluoZin-3 at 530 nm (Fig. 2*C*). Coincubation of cultures with 50 to 100 μmol/L zinc acetate and MGd led to synergistic increases in the corresponding fluorescent signals. Next, we attempted to

determine the mechanisms by which MGd treatment alters levels of free intracellular zinc. Cells were incubated in the complete absence of exogenous zinc (serum-free medium) to evaluate the role zinc uptake plays in this process. Cells were also treated with actinomycin D to minimize the expression of genes (i.e., metallothionein family members and *ZnT1*) that might mask drug-induced changes in free intracellular zinc levels. Interestingly, cotreatment of cells with MGd and actinomycin D lead to a 1.5-fold increase in cellular fluorescence (Fig. 2*C*, *inset*). No increase in cellular fluorescence at 530 nm was observed in the absence of FluoZin-3 in these experiments.

Effect of motexafin gadolinium on the antiproliferative effects of zinc acetate. To determine whether MGd modulation of metal ion availability was restricted to quiescent cell cultures, exponential growth phase A549 cultures were treated with zinc in the presence or absence of MGd for 24 hours. After an additional 48 hour growth period, viable cells were measured using a tetrazole reduction assay. Zinc treatment modestly inhibited A549 cell proliferation at the highest (100 μmol/L) concentration. Treatment with MGd alone had no effect on proliferation, but enhanced the antiproliferative activity of zinc at all MGd concentrations tested (Fig. 2*D*).

Motexafin gadolinium modulation of zinc activity in PC3 prostate cancer cells and Ramos lymphoma cells. Treatment of plateau phase PC3 cultures with zinc had little effect on cell viability after 24 hours (data not shown), but increased cell death (2-fold at 100 μmol/L zinc), as measured by propidium iodide exclusion, was apparent within 48 hours (Fig. 3*A*). MGd enhanced the cytotoxic effect of zinc (e.g., 5-fold at 100 μmol/L zinc), similar to what was observed in the A549 line. Metallothionein and *ZnT1* levels were elevated after treatment with MGd and zinc (Fig. 3*B*). As before, treatment with MGd led to increased zinc-associated cellular fluorescence in the presence of exogenous zinc (Fig. 3*C*). Indeed, in this cell line, incubation with MGd alone led to a more marked increase in cellular fluorescence after 4 hours (~2-fold) than in A549. Interestingly, PC3 cell proliferation was also inhibited by zinc (Fig. 3*D*). As in the A549 line, treatment with MGd enhanced the effect of zinc. This effect was confirmed by colony-forming assay. A surviving fraction of 0.16 was measured in the presence of 10 μmol/L MGd and 75 μmol/L zinc, whereas zinc or MGd alone was without effect (data not shown).

Furthermore, we examined the effect of MGd and zinc treatment on viability, metallothionein and *ZnT1* gene expression, and intracellular levels of free zinc in Ramos B-cell lymphoma cells grown in suspension (Fig. 4*A-C*). Overall, the results were qualitatively similar to those obtained with A549 and PC3, with the difference that changes were generally observed at lower

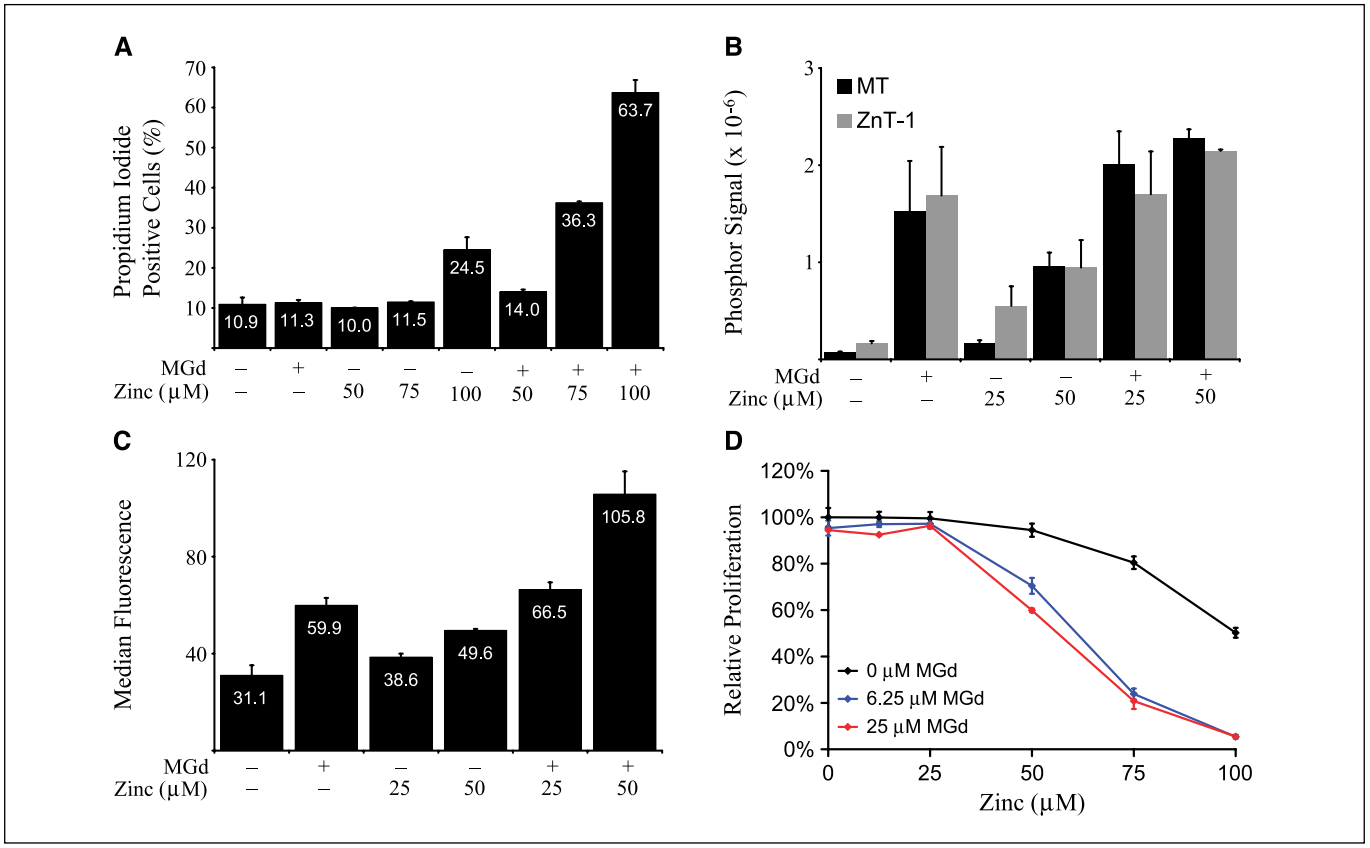

Figure 3. MGd treatment alters response of PC3 cells to zinc. *A,* cell viability as measured by propidium iodide exclusion. Plateau phase cultures were treated with zinc acetate (*Zinc*, 50-100 μmol/L) or MGd (50 μmol/L) for 48 hours in duplicate experiments. *Bars,* 1 SD. *B,* transcript levels of metallothionein family members and *ZnT1* in PC3 cultures treated with MGd (50 μmol/L) and zinc acetate (25-50 μmol/L) for 4 hours as determined by Northern blot analysis. Phosphorimager signals from metallothionein family members were normalized to those of internal β-actin controls. *C,* measurement of intracellular free zinc in PC3 cells. Plateau phase cultures were treated with zinc acetate (25-50 μmol/L) or MGd (50 μmol/L) for 4 hours in duplicate experiments. Median fluorescence at 530 nm of cells treated with FluoZin-3, as described in Materials and Methods. *Bars,* SD. *D,* effect of MGd and zinc treatment on proliferation of PC3 cells. Exponential growth phase cultures were treated with MGd (0, 6.25, and 25 μmol/L) and zinc (0-100 μmol/L) for 24 hours as described in the caption to Fig. 2. Cells treated with 12.5 and 18.75 μmol/L MGd behaved in a similar fashion to those treated with 25 μmol/L MGd (data not shown).

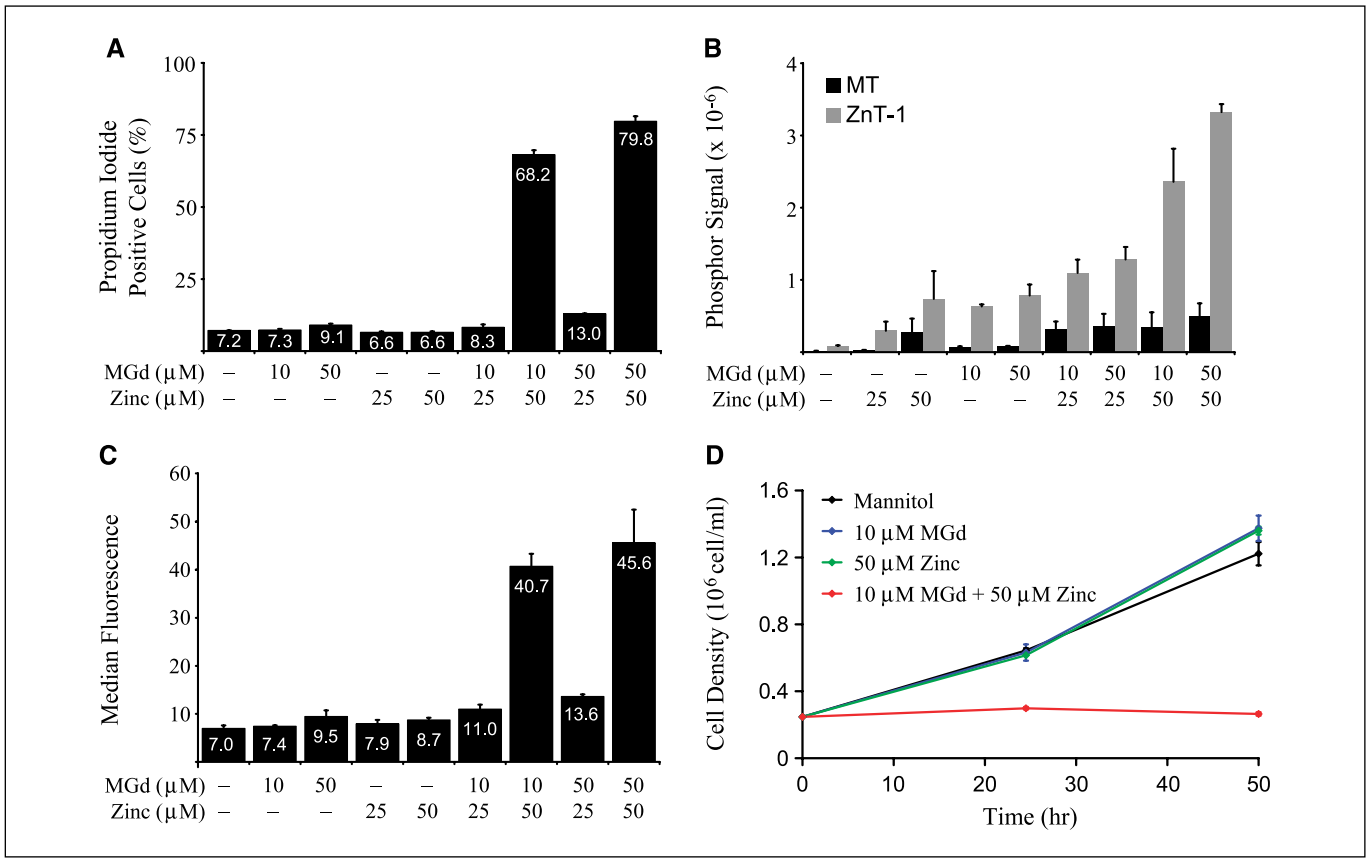

Figure 4. Effects of combined MGd and zinc treatment in Ramos cells. Exponential growth phase Ramos cell cultures were treated with zinc acetate (25 or 50 μmol/L) or MGd (10 μmol/L or 50 μmol/L) for 24 hours (*A*), 6 hours (*B* and *C*), or 48 hours (*D*) and assayed for (*A*) viability, (*B*) metallothionein family member and *ZnT1* RNA transcript levels, (*C*) FluoZin-3 fluorescence, (*D*) proliferation. *D,* treatment with 25 μmol/L zinc with or without MGd (25 or 50 μmol/L) had no effect on proliferation (data not shown). Also in (*D*), cotreatment with 50 μmol/L zinc and 50 μmol/L MGd completely inhibited proliferation (data not shown). *Bars,* 1 SD.

(i.e., 25-50 μmol/L) concentrations of zinc. Cellular proliferation was strongly inhibited by 50 μmol/L zinc and MGd, whereas either agent alone was without effect (Fig. 4*D*).

Inhibition of lipoate reduction. We previously reported that MGd caused an increase in radiation response in A549 cultures treated with BSO, an inhibitor of glutathione synthesis (21). This observation led us to investigate the effect of MGd treatment on the complementary, glutathione-independent thioredoxin pathway. Thioredoxin reductase activity can be evaluated in intact cells by measuring the reduction of the oxidized form of the cell-permeable cofactor lipoate to its reduced form, dihydrolipoate (28). Using this method, we observed a modest (~10%) inhibition of lipoate reduction in plateau phase A549 cultures after a 2-hour treatment with MGd alone (Fig. 5*A*). Moreover, up to a 30% inhibition of lipoate reduction was observed after treatment of cultures with zinc alone, consistent with literature reports of thioredoxin reductase inhibition by this cation (39–41). Greater inhibition (up to 60%) was observed after treatment with both zinc and MGd (Fig. 5*A*). This effect of MGd was dose dependent, with an apparent inhibitory concentration of ~2.5 μmol/L. The inhibition of lipoate reduction was less pronounced (~30%) after 4 hours of incubation (Fig. 5*B*). Pretreatment with either actinomycin D (Fig. 5*C*) or cycloheximide (data not shown) restored the inhibitory effect of both MGd and zinc on lipoate reduction. These findings lead us to suggest that A549 cells compensate for increases in intracellular zinc levels by transcription and translation-dependent processes. Lipoate reduction was also inhibited in cells treated with zinc 1-hydroxypyridine-2-thiol, a zinc ionophore that increases the concentration of intracellular zinc (Fig. 5*D*). Preincubation of cultures with the glutathione synthesis inhibitor BSO increased the degree of inhibition by MGd and zinc, demonstrating that both agents were targeting the glutathione-independent lipoate reduction pathway (data not shown; ref. 28). Similar observations were obtained using plateau phase PC3 prostate cancer cell cultures (Fig. 5*E-H*). However, lipoate reduction was inhibited at lower concentrations of zinc in PC3 cells as compared with A549. Lipoate reduction was similarly inhibited by MGd and zinc in exponential Ramos lymphoma cultures (data not shown).

Discussion

We examined the effect of MGd treatment on mRNA levels in A549 lung cancer cell cultures at multiple exposure times and observed a highly specific response that consisted of a strong and sustained induction of metallothionein and *ZnT1* transcripts (Table 1). Metallothioneins possess multiple cysteine-rich sites that can bind metal cations. They are expressed constitutively and may be further induced by toxic metal cations such as Cd(II) or by nontoxic cations such as Zn(II) (3–5). ZnT1 is a plasma membrane–bound protein that transports zinc to the outside of the cell (4, 11, 42, 43). The transcription of metallothionein genes

and *ZnT1* is induced by MTF-1 (31–34), a metal-dependent transactivator that binds to metal response elements located in the promoters of metallothionein and other genes (Fig. 1*C*; refs. 31–34).

Initially, displacement of zinc by free Gd(III) was considered as a possible explanation for the observed metallothionein induction (e.g., gadolinium chloride treatment has been reported to induce metallothionein expression in rat liver; ref. 35). However, the lack of metallothionein induction by free gadolinium as assessed by Northern blot analysis (Fig. 1*B*) is not consistent with this explanation. Moreover, stability studies indicate that release of free Gd(III) from MGd is unlikely (data not shown). We therefore considered other pathways by which metallothionein induction could occur.

Zinc metallothioneins are believed to be a major site of intracellular zinc storage and transport (3–5, 31–34). As shown in Fig. 1*C*, oxidation of zinc metallothionein by hydrogen peroxide leads to the formation of thionein and the release of zinc (44–46). The disulfide bond in thionein must be reduced by thioredoxin reductase in order to recoordinate to zinc. The released zinc can bind and activate MTF-1, leading, in turn, to up-regulation of thionein expression (44–46). The binding of zinc by the newly

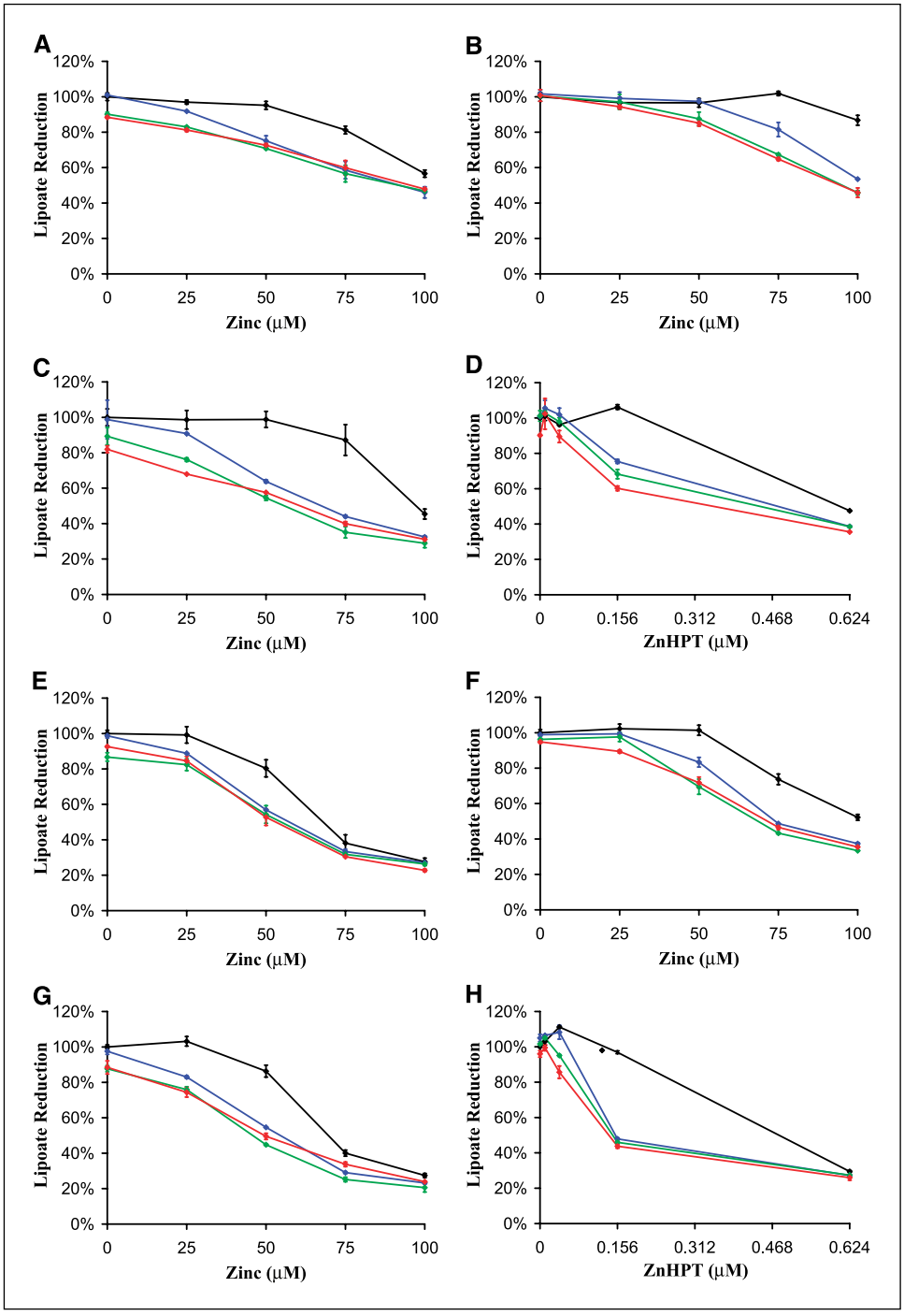

Figure 5. Lipoate reduction in A549 and PC3 cells. Plateau phase A549 (*A-D*) and PC3 (*E-H*) cultures were treated with zinc acetate (0-100 μmol/L) or zinc 1-hydroxy-2-pyridinethione (*ZnHPT*, 0-0.624 μmol/L) and MGd [0 (*black line*), 2.5 (*blue line*), 5 (*green line*), and 10 μmol/L (*red line*)], medium exchanged, and relative lipoate reduction measured after 20-40 minutes) as described in Materials and Methods. *A* and *E*, 2-hour treatment. *B* and *F*, 4- or 3-hour treatment, respectively. *C* and *G*, as in (*B*) and (*F*), except actinomycin D (2.5 μg/mL) was added to cultures 1 hour before MGd or zinc. *D* and *H*, cultures coincubated with MGd and ZnHPT for 4 hours. *Bars*, 1 SD, although not readily visible due to the reproducibility of the data.

transcribed thioneins provides a negative feedback mechanism for metallothionein expression.

MGd is a redox active agent that has been shown to redox cycle and form reactive oxygen species in cells (20–23). Other redox cycling agents have been shown to induce metallothionein expression (36). Interestingly, recent data suggests that MGd oxidizes vicinal thiols such as dithiothreitol and can inhibit thioredoxin reductase (22). It is therefore possible that the generation of reactive oxygen species, the direct oxidation of zinc metallothionein by the complex, or thioredoxin reductase inhibition could be responsible for the observed metallothionein induction. However, MGd treatment affects only a subset of the genes reported to be induced or repressed by oxidative stress in cultured mammalian cells (47–52). This could be due to differences in the cell lines and growth conditions examined or the possible targeted nature of MGd action.

Treatment with MGd attenuated the cytotoxicity of cadmium chloride and potentiated that of zinc acetate in A549 cells (Fig. 2*A*). Metallothionein transcript levels were raised by treatment with MGd, zinc, cadmium, or combinations of these species (Fig. 2*B*). Attenuated cadmium toxicity is consistent with literature reports of protection from cadmium chloride toxicity by metallothionein induction (37, 38). Enhanced zinc toxicity, however, is inconsistent with a recent report of the protection of baby hamster kidney cells against zinc toxicity by metallothionein and zinc transporter 1 (43). In an effort to resolve this apparent contradiction, we examined intracellular levels of free zinc using the ion-specific probe, FluoZin-3 (K_d = 15 nmol/L; ref. 29), and observed significantly (at least 2.4-fold) increased cellular fluorescence signals after coincubation with MGd and 50 to 100 μmol/L zinc for 4 hours (Fig. 2*C*). Synergistic increases in intracellular free zinc levels in response to coincubation with MGd and zinc acetate could explain the cellular toxicity observed. Furthermore, the 1.5-fold increase in cellular fluorescence signal observed by coincubating A549 cells with MGd and actinomycin D in zinc-free medium (Fig. 2*C*, *inset*) suggests that MGd treatment can mobilize bound intracellular zinc. This mobilization is normally quenched by cellular gene expression responses, most likely those of metallothionein gene family members and *ZnT1* because MGd treatment in the absence of actinomycin D only led to marginal increases in cellular fluorescence in both serum and serum-free media (1.2- and 1.1-fold, respectively, in A549).

Similar effects were observed in PC3 prostate cancer and Ramos B-cell lymphoma cell lines. Combined treatment with MGd and zinc led to increased cell death after 48 hours in PC3 cultures (Fig. 3*A*) and after 24 hours in Ramos cultures (Fig. 4*A*). Expression of metallothionein family members and *ZnT1* were increased by MGd in both lines (Figs. 3*B* and 4*B*). Larger changes in FluoZin-3 fluorescence (~2-fold) were observed in PC3 cultures treated with MGd alone than in the A549 or Ramos lines (Figs. 2*C*, 3*C*, and 4*C*). The difference could result from the lesser induction of gene expression of metallothionein gene family members or *ZnT1* in this line (4).

Increased intracellular zinc levels would also explain the effect of MGd and zinc on lipoate reduction (Fig. 5). Lipoate is mainly reduced by thioredoxin reductase in mammalian cells, accounting for approximately two thirds of this activity in A549 cultures, with the remainder due to glutaredoxin or other enzymes (28, 53). Inhibition of thioredoxin reductase by zinc in cell extracts was reported previously (40, 41). The data in Fig. 5 show that zinc inhibition of thioredoxin reductase occurs in intact cells. MGd alone had a modest effect on the rate of lipoate reduction under our conditions after 2 hours of treatment (Fig. 5*A*, *y axis*). Moreover, inhibition of lipoate reduction by zinc was potentiated by MGd. The effect of MGd was dose dependent and saturated above a concentration of ~5 μmol/L. The inhibition of lipoate reduction was less pronounced after 4 hours of incubation (Fig. 5*B*). However, pretreatment with either actinomycin D (Fig. 5*C*) or cycloheximide (data not shown) restored the inhibitory effect of both MGd and zinc. This is reminiscent of the effect of actinomycin D on the fluorescence measurements described above (Fig. 2*C*) and is consistent with compensatory cellular RNA and protein expression in response to MGd. Lipoate reduction was also inhibited in cells treated with a zinc ionophore (Fig. 5*D*), demonstrating that the effect of MGd was independent of the mode of zinc uptake. Lipoate reduction was similarly inhibited by zinc and MGd in PC3 and Ramos cultures (Fig. 5*E-H* and data not shown).

Thioredoxin reductase is an important component of the cellular antioxidant system and is involved in a variety of other processes including apoptotic signaling and DNA synthesis (54). It has recently been highlighted as an attractive target for anticancer agent activity (55). In the present study, combined treatment with MGd and zinc inhibited cell proliferation (Figs. 2*D*, 3*D*, and 4*D*) and led to cell death (Figs. 2*A*, 3*A*, and 4*A*). Similar observations were made using the HF-1 and DHL-4 B-lymphoma cell lines (data not shown). Thioredoxin reductase inhibition could contribute to the observed effects.

Of course, many other proteins require zinc for activity and may therefore be affected by changes in the intracellular concentration of available zinc. The observation of a sustained induction of *ZnT1* and metallothionein transcripts suggests a corresponding increase in the intracellular availability of zinc during drug treatment. MGd could therefore modulate a variety of downstream processes by mobilizing zinc. The importance of this would likely depend on the particular system under study but would be most likely to occur in tumors, where the drug seems to localize selectively (15–19).

Because zinc treatments were reported to inhibit tumor growth in animal models in 1969 (56), there has been considerable interest in the role of zinc in cancer development and progression (2, 57–59). MGd represents a novel class of compounds capable of altering the expression of MTF-1 responsive genes and altering zinc homeostasis in cancer cells. Therefore, MGd could be a valuable experimental tool to examine the role of zinc in the control of transcription and metabolic pathways. Furthermore, studies are under way to examine MTF-1 responsive genes as surrogate markers for the biological activity of MGd. Finally, the above findings provide support for the hypothesis that agents that increase intracellular zinc levels have potential applications as anticancer therapeutics.

Acknowledgments

Received 11/15/2004; revised 1/20/2005; accepted 2/8/2005.

Grant support: Donald E. and Delia B. Baxter Foundation (J.G. Hacia) and the V Foundation for Cancer Research (J.G. Hacia).

The costs of publication of this article were defrayed in part by the payment of page charges. This article must therefore be hereby marked *advertisement* in accordance with 18 U.S.C. Section 1734 solely to indicate this fact.

We thank Juergen Reichardt at the University of Southern California for critical insights and discussion.

References

1. Leonard SS, Bower JJ, Shi X. Metal-induced toxicity, carcinogenesis, mechanisms and cellular responses. Mol Cell Biochem 2004;255:3–10.
2. Leitzmann MF, Stampfer MJ, Wu K, Colditz GA, Willett WC, Giovannucci EL. Zinc supplement use and risk of prostate cancer. J Natl Cancer Inst 2003;95:1004–7.
3. Cherian MG, Jayasurya A, Bay BH. Metallothioneins in human tumors and potential roles in carcinogenesis. Mutat Res 2003;533:201–9.
4. Hasumi M, Suzuki K, Matsui H, Koike H, Ito K, Yamanaka H. Regulation of metallothionein and zinc transporter expression in human prostate cancer cells and tissues. Cancer Lett 2003;200:187–95.
5. Jayasurya A, Bay BH, Yap WM, Tan NG, Tan BK. Proliferative potential in nasopharyngeal carcinoma: correlations with metallothionein expression and tissue zinc levels. Carcinogenesis 2000;21:1809–12.
6. Kondoh M, Tasaki E, Araragi S, et al. Requirement of caspase and p38MAPK activation in zinc-induced apoptosis in human leukemia HL-60 cells. Eur J Biochem 2002;269:6204–11.
7. Kim CH, Kim JH, Moon SJ, et al. Pyrithione, a zinc ionophore, inhibits NF-κB activation. Biochem Biophys Res Commun 1999;259:505–9.
8. Seo SR, Chong SA, Lee SI, et al. Zn^{2+}-induced ERK activation mediated by reactive oxygen species causes cell death in differentiated PC12 cells. J Neurochem 2001;78:600–10.
9. Forbes IJ, Zalewski PD, Giannakis C. Role for zinc in a cellular response mediated by protein kinase C in human B lymphocytes. Exp Cell Res 1991;195:224–9.
10. Uzzo RG, Leavis P, Hatch W, et al. Zinc inhibits nuclear factor-κB activation and sensitizes prostate cancer cells to cytotoxic agents. Clin Cancer Res 2002;8:3579–83.
11. Cousins RJ, Blanchard RK, Popp MP, et al. A global view of the selectivity of zinc deprivation and excess on genes expressed in human THP-1 mononuclear cells. Proc Natl Acad Sci U S A 2003;100:6952–7.
12. Hecht D, Jung D, Prabhu VV, Munson PJ, Hoffman MP, Kleinman HK. Metallothionein promotes laminin-1-induced acinar differentiation *in vitro* and reduces tumor growth *in vivo*. Cancer Res 2002;62:5370–4.
13. Zhang CX, Lippard SJ. New metal complexes as potential therapeutics. Curr Opin Chem Biol 2003;7:481–9.
14. Ramotar D, Wang H. Protective mechanisms against the antitumor agent bleomycin: lessons from *Saccharomyces cerevisiae*. Curr Genet 2003;43:213–24.
15. Rosenthal DI, Nurenberg P, Becerra CR, et al. A phase I single-dose trial of gadolinium texaphyrin (Gd-Tex), a tumor selective radiation sensitizer detectable by magnetic resonance imaging. Clin Cancer Res 1999;5:739–45.
16. Carde P, Timmerman R, Mehta MP, et al. Multicenter phase Ib/II trial of the radiation enhancer motexafin gadolinium in patients with brain metastases. J Clin Oncol 2001;19:2074–83.
17. Mehta MP, Shapiro WR, Glantz MJ, et al. Lead-in phase to randomized trial of motexafin gadolinium and whole-brain radiation for patients with brain metastases: centralized assessment of magnetic resonance imaging, neurocognitive, and neurologic end points. J Clin Oncol 2002;20:3445–53.
18. Mehta MP, Rodrigus P, Terhaard CH, et al. Survival and neurologic outcomes in a randomized trial of motexafin gadolinium and whole-brain radiation therapy in brain metastases. J Clin Oncol 2003;21:2529–36.
19. Rodrigus P. Motexafin gadolinium: a possible new radiosensitiser. Expert Opin Investig Drugs 2003;12:1205–10.
20. Magda D, Gerasimchuk N, Lecane P, Miller RA, Biaglow JE, Sessler JL. Motexafin gadolinium reacts with ascorbate to produce reactive oxygen species. Chem Commun (Camb) 2002;22:2730–1.
21. Magda D, Lepp C, Gerasimchuk N, et al. Redox cycling by motexafin gadolinium enhances cellular response to ionizing radiation by forming reactive oxygen species. Int J Radiat Oncol Biol Phys 2001;51:1025–36.
22. Biaglow JE, Miller RA, Magda D, Lee I, Tuttle S. Inhibition of thioredoxin reductase by motexafin gadolinium: effects on PLDR. Prog Abst Radiat Res Soc 2002:107.
23. Rockwell S, Donnelly ET, Liu Y, Tang LQ. Preliminary studies of the effects of gadolinium texaphyrin on the growth and radiosensitivity of EMT6 cells *in vitro*. Int J Radiat Oncol Biol Phys 2002;54:536–41.
24. Varnes ME, Menegay HJ, McKenna DS. Inhibition of recovery from potentially lethal radiation damage in A549 cells by the K^+/H^+ ionophore nigericin. Int J Radiat Oncol Biol Phys 1991;20:281–5.
25. Karaman MW, Houck ML, Chemnick LG, et al. Comparative analysis of gene-expression patterns in human and African great ape cultured fibroblasts. Genome Res 2003;13:1619–30.
26. Tusher VG, Tibshirani R, Chu G. Significance analysis of microarrays applied to the ionizing radiation response. Proc Natl Acad Sci U S A 2001;98:5116–21.
27. Mosmann T. Rapid colorimetric assay for cellular growth and survival: application to proliferation and cytotoxicity assays. J Immunol Methods 1983;65:55–63.
28. Biaglow JE, Donahue J, Tuttle S, Held K, Chrestensen C, Mieyal J. A method for measuring disulfide reduction by cultured mammalian cells: relative contributions of glutathione-dependent and glutathione-independent mechanisms. Anal Biochem 2000;281:77–86.
29. Gee KR, Zhou ZL, Ton-That D, Sensi SL, Weiss JH. Measuring zinc in living cells. A new generation of sensitive and selective fluorescent probes. Cell Calcium 2002;31:245–51.
30. Takeda J, Yano H, Eng S, Zeng Y, Bell GI. A molecular inventory of human pancreatic islets: sequence analysis of 1000 cDNA clones. Hum Mol Genet 1993;2:1793–8.
31. Giedroc DP, Chen X, Apuy JL. Metal response element (MRE)-binding transcription factor-1 (MTF-1): structure, function, and regulation. Antioxid Redox Signal 2001;3:577–96.
32. Lichtlen P, Schaffner W. Putting its fingers on stressful situations: the heavy metal-regulatory transcription factor MTF-1. Bioessays 2001;23:1010–7.
33. Lichtlen P, Wang Y, Belser T, et al. Target gene search for the metal-responsive transcription factor MTF-1. Nucleic Acids Res 2001;29:1514–23.
34. Andrews GK. Cellular zinc sensors: MTF-1 regulation of gene expression. Biometals 2001;14:223–37.
35. Sauer JM, Waalkes MP, Hooser SB, Kuester RK, McQueen CA, Sipes IG. Suppression of Kupffer cell function prevents cadmium induced hepatocellular necrosis in the male Sprague-Dawley rat. Toxicology 1997;121:155–64.
36. Andrews GK. Regulation of metallothionein gene expression by oxidative stress and metal ions. Biochem Pharmacol 2000;59:95–104.
37. Nordberg GF. Modulation of metal toxicity by metallothionein. Biol Trace Elem Res 1989;21:131–5.
38. Achanzar WE, Achanzar KB, Lewis JG, Webber MM, Waalkes MP. Cadmium induces c-myc, p53, and c-jun expression in normal human prostate epithelial cells as a prelude to apoptosis. Toxicol Appl Pharmacol 2000;164:291–300.
39. Holmgren A. Thioredoxin. Annu Rev Biochem 1985;54:237–71.
40. Lenartowicz E, Wudarczyk J. Enzymatic reduction of 5,5′-dithiobis-(2-nitrobenzoic acid) by lysate of rat liver mitochondria. Int J Biochem Cell Biol 1995;27:831–7.
41. Rigobello MP, Callegaro MT, Barzon E, Benetti M, Bindoli A. Purification of mitochondrial thioredoxin reductase and its involvement in the redox regulation of membrane permeability. Free Radic Biol Med 1998;24:370–6.
42. Langmade SJ, Ravindra R, Daniels PJ, Andrews GK. The transcription factor MTF-1 mediates metal regulation of the mouse ZnT1 gene. J Biol Chem 2000;275:34803–9.
43. Palmiter RD. Protection against zinc toxicity by metallothionein and zinc transporter 1. Proc Natl Acad Sci U S A 2004;101:4918–23.
44. Zhang B, Georgiev O, Hagmann M, et al. Activity of metal-responsive transcription factor 1 by toxic heavy metals and H_2O_2 *in vitro* is modulated by metallothionein. Mol Cell Biol 2003;23:8471–85.
45. Maret W, Vallee BL. Thiolate ligands in metallothionein confer redox activity on zinc clusters. Proc Natl Acad Sci U S A 1998;95:3478–82.
46. Jacob C, Maret W, Vallee BL. Control of zinc transfer between thionein, metallothionein, and zinc proteins. Proc Natl Acad Sci U S A 1998;95:3489–94.
47. Murray JI, Whitfield ML, Trinklein ND, Myers RM, Brown PO, Botstein D. Diverse and specific gene expression responses to stresses in cultured human cells. Mol Biol Cell 2004;15:2361–74.
48. Yoneda K, Chang MM, Chmiel K, Chen Y, Wu R. Application of high-density DNA microarray to study smoke- and hydrogen peroxide-induced injury and repair in human bronchial epithelial cells. J Am Soc Nephrol 2003;14:S284–9.
49. Weigel AL, Handa JT, Hjelmeland LM. Microarray analysis of H_2O_2-, HNE-, or tBH-treated ARPE-19 cells. Free Radic Biol Med 2002;33:1419–32.
50. Chuang YY, Chen Y, Gadisetti, et al. Gene expression after treatment with hydrogen peroxide, menadione, or *t*-butyl hydroperoxide in breast cancer cells. Cancer Res 2002;62:6246–54.
51. Morgan KT, Ni H, Brown HR, et al. Application of cDNA microarray technology to *in vitro* toxicology and the selection of genes for a real-time RT-PCR-based screen for oxidative stress in Hep-G2 cells. Toxicol Pathol 2002;30:435–51.
52. Suzuki T, Spitz DR, Gandhi P, Lin HY, Crawford DR. Mammalian resistance to oxidative stress: a comparative analysis. Gene Expr 2002;10:179–91.
53. Arner ES, Nordberg J, Holmgren A. Efficient reduction of lipoamide and lipoic acid by mammalian thioredoxin reductase. Biochem Biophys Res Commun 1996;225:268–74.
54. Arner ES, Holmgren A. Physiological functions of thioredoxin and thioredoxin reductase. Eur J Biochem 2000;267:6102–9.
55. Smart DK, Ortiz KL, Mattson D, et al. Thioredoxin reductase as a potential molecular target for anticancer agents that induce oxidative stress. Cancer Res 2004;64:6716–24.
56. Cherkasova EV. The effect of zinc on oxygen consumption, phagocytosis and the development of Pliss lymphosarcoma. Vopr Onkol 1969;15:81–5.
57. Liang JY, Liu YY, Zou J, Franklin RB, Costello LC, Feng P. Inhibitory effect of zinc on human prostatic carcinoma cell growth. Prostate 1999;40:200–7.
58. Feng P, Li TL, Guan ZX, Franklin RB, Costello LC. Effect of zinc on prostatic tumorigenicity in nude mice. Ann N Y Acad Sci 2003;1010:316–20.
59. Yin H, Smith M, Glass J. Stable expression of C/EBPα in prostate cancer cells down-regulates metallothionein and increases zinc-induced toxicity. Prostate 2005;62:209–16.